

Spectral amplitude and phase measurement of a 40 GHz free-running quantum-dash modelocked laser diode

S. G. Murdoch,^{1,*} R. T. Watts,² Y. Q. Xu,¹ R. Maldonado-Basilio,² J. Parra-Cetina,²
S. Latkowski,² P. Landais,² and L. P. Barry²

¹Physics Department, University of Auckland, Private Bag 92019, Auckland, New Zealand

²Research Institute for Networks and Communications Engineering, School of Electronic Engineering, Dublin City University, Dublin 9, Ireland

*s.murdoch@auckland.ac.nz

Abstract: We present a linear self-referenced measurement of the spectral amplitude and phase of a free-running quantum-dash modelocked laser diode. The technique is suitable for measuring optical signals with repetition rates up to 100 GHz. In contrast to many other linear techniques it requires no external electronic clock synchronized to the signal under test. Using this method we are able to compensate for the intracavity dispersion of the diode to demonstrate 500 fs pulses at a repetition rate of 39.8 GHz. We also use the technique to characterize the dependence of the diode's intracavity dispersion on the applied current.

©2011 Optical Society of America

OCIS codes: (140.5960) Semiconductor lasers; (140.7090) Ultrafast lasers; (190.5970) Semiconductor nonlinear optics including MQW.

References and links

1. F. Lelarge, B. Dagens, J. Renaudier, R. Brenot, A. Accard, F. Dijk, D. Make, O. L. Gouezigou, J.-G. Provost, F. Poingt, J. Landreau, O. Drisse, E. Derouin, B. Rousseau, F. Pommereau, and G.-H. Duan, "Recent advances on InAs/InP quantum dash based semiconductor lasers and optical amplifiers operating at 1.55 μm ," *IEEE J. Sel. Top. Quantum Electron.* **13**(1), 111–124 (2007).
2. G.-H. Duan, A. Shen, A. Akrouf, F. V. Dijk, F. Lelarge, F. Pommereau, O. LeGouezigou, J.-G. Provost, H. Gariah, F. Blache, F. Mallecot, K. Merghem, A. Martinez, and A. Ramdane, "High performance InP-based quantum dash semiconductor mode-locked lasers for optical communications," *Bell Labs Tech. J.* **14**(3), 63–84 (2009).
3. D. A. Reid, S. G. Murdoch, and L. P. Barry, "Stepped-heterodyne optical complex spectrum analyzer," *Opt. Express* **18**(19), 19724–19731 (2010).
4. A. Shen, J. G. Provost, A. Akrouf, B. Rousseau, F. Lelarge, O. Legouezigou, F. Pommereau, F. Poingt, L. Legouezigou, G. H. Duan, and A. Ramdane, "Low confinement factor quantum dash (QD) mode-locked Fabry-Perot (FP) laser diode for tunable pulse generation," *Optical Fiber Communications Conference, OThK1* (2008).
5. A. Akrouf, A. Shen, F. Lelarge, F. Pommereau, H. Gariah, F. Blache, G. H. Duan, and A. Ramdane, "Spectrum Filtering and Pulse Compression of Quantum-Dash Mode-Locked Lasers Emitting at 1.55 μm ," *Proc. 34th Eur. Conf. on Optical Commun.*, P2.20 (2008).
6. X. Tang, A. S. Karar, J. C. Cartledge, A. Shen, and G. H. Duan, "Characterization of a mode-locked quantum-dash Fabry-Perot laser based on measurement of the complex optical spectrum," *Proc. 35th Eur. Conf. on Optical Commun.* P2.21 (2009).
7. C. Gosset, K. Merghem, G. Moreau, A. Martinez, G. Aubin, J.-L. Oudar, A. Ramdane, and F. Lelarge, "Phase-amplitude characterization of a high-repetition-rate quantum dash passively mode-locked laser," *Opt. Lett.* **31**(12), 1848–1850 (2006).
8. N. G. Usechak, Yongchun Xin, Chang-Yi Lin, L. F. Lester, D. J. Kane, and V. Kovanis, "Modeling and direct electric-field measurements of passively mode-locked quantum-dot lasers," *IEEE J. Sel. Top. Quantum Electron.* **15**(3), 653–660 (2009).
9. S. Latkowski, R. Maldonado-Basilio, and P. Landais, "Sub-picosecond pulse generation by 40-GHz passively mode-locked quantum-dash 1-mm-long Fabry-Pérot laser diode," *Opt. Express* **17**(21), 19166–19172 (2009).
10. J. Debeau, B. Kowalski, and R. Boittin, "Simple method for the complete characterization of an optical pulse," *Opt. Lett.* **23**(22), 1784–1786 (1998).
11. M. Kwakernaak, R. Schreieck, A. Neiger, H. Jackel, E. Gini, and W. Vogt, "Spectral phase measurement of mode-locked diode laser pulses by beating sidebands generated by electrooptical mixing," *IEEE Photon. Technol. Lett.* **12**(12), 1677–1679 (2000).

12. C. Dorrer and I. Kang, "Linear self-referencing techniques for short-optical-pulse characterization," *J. Opt. Soc. Am. B* **25**(6), A1–A12 (2008).
 13. J. Renaudier, G. H. Duan, P. Landais, and P. Gallion, "Phase correlation and linewidth reduction of 40 GHz self-pulsation in distributed Bragg reflector semiconductor lasers," *IEEE J. Quantum Electron.* **43**(2), 147–156 (2007).
-

1. Introduction

Modelocked laser diodes have the ability to generate sub-picosecond optical pulses at very high repetition rates. As such they are ideally suited for use in time-division-multiplexed optical communication channels, all-optical clock recovery, optical sampling, and the generation of THz radiation [1,2]. In this letter we report on the measurement of the spectral amplitude and phase of the output of a free-running quantum-dash modelocked laser diode (QD-MLLD). This measurement allows the complete characterization of the temporal and spectral properties of the device. From these measurements we show how passive dispersion compensation can be used to obtain a clean train of 500 fs pulses at a repetition rate of 39.8 GHz. The measurement is an extension of the stepped-heterodyne method presented in [3]. We show how the addition of an electronic local oscillator to the setup allows the measurement of signals with repetition rates up to 100 GHz. Previous measurements of the spectral amplitude and phase of quantum-dash and quantum-dot modelocked laser diodes have been reported using both linear [4–6] and nonlinear techniques [7–9]. Typically linear methods possess a better sensitivity and dynamic range than the nonlinear methods [10–12]. The linear methods presented in [4–6] all require an external electronic clock synchronized to the optical signal under test in order to operate correctly. For a passively modelocked laser diode where the repetition rate is set simply by the length of the diode cavity an external clock recovery circuit is necessary to provide this synchronization signal. A key advantage of the method presented in this letter is that it does not require any synchronized external electronic clock. This, in addition to the high sensitivity possible with a heterodyne measurement, makes it ideally suited to the measurement of free-running modelocked laser diodes.

2. Measurement technique

The laser we wish to characterize is a passively modelocked quantum-dash Fabry-Perot laser diode. It consists of a single, DC-biased, 1 mm long, active section with no saturable absorber. A more detailed description of the geometry and material composition of the device is given in [9]. The modelocking mechanism is phase-sensitive four-wave-mixing which phase locks the longitudinal modes of the cavity [13]. The optical spectrum of the laser diode consists of ~50 spectral lines of roughly equal power, each spaced by 39.8 GHz, spanning a wavelength range from 1515 to 1530 nm. This wavelength range, and the low output power of the device (~2 mW average power), makes nonlinear measurements like frequency-resolved-optical-gating (FROG) very difficult. Previously reported FROG measurements of this device required the use of an EDFA in order to obtain a sufficiently high signal power to experimentally record a FROG trace [9]. As a significant part of the laser's spectrum falls outside the EDFA's gain band considerable spectral distortion results. The recovered FROG trace from such a signal is not an accurate representation of the optical signal emerging directly from the laser diode. The use of a linear technique removes the need for optical amplification, allowing a direct measurement of the spectral amplitude and phase of the optical signal exiting the diode. The signal under test is mixed with a narrowband tunable CW optical local oscillator. The local oscillator is positioned between a pair of signal modes and the combined signal is incident on a photodiode. The detected photocurrent contains the beat frequencies between the local oscillator and the two signal modes under interrogation, as well as the fundamental beat frequency of the signal modes. In [3] this signal was then recorded directly on a real-time oscilloscope. This limited the maximum repetition rate of the signal under test to the bandwidth of the real-time scope. In this paper we show how, with the addition of a mixer and electronic local oscillator, beat frequencies that fall outside the bandwidth of the real-time scope can be electronically heterodyned back down into the scope's bandwidth without affecting the measurement. This lifts the maximum repetition of a

signal measurable using this technique to that of the bandwidth of the photo-receiver used, rather than that of the real-time scope. In principle this means repetition rates up to 100 GHz should be readily measurable using this technique. The recorded signal is then analyzed to extract the amplitude of each of the two signal modes as well as the phase difference between them. The full measurement then consists of stepping the optical local oscillator across all signal modes, and repeating this measurement at each point. This yields a complete characterization of the signal's spectral amplitude and phase, and via a Fourier transform a complete characterization of the signal's temporal amplitude and phase.

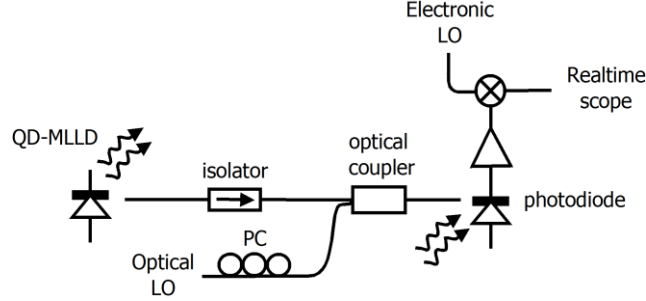


Fig. 1. Schematic diagram of the experimental setup.

The experimental setup for the measurement is shown in Fig. 1. The optical signal exiting the QD-MLLD passes through a 50 dB isolator before being mixed with the optical local oscillator, a tunable external cavity laser (linewidth ~ 100 kHz), using a fused-fiber coupler. A polarization controller is used to ensure the polarization of the local oscillator is collinear with that of the signal from the QD-MLLD. This mixed signal is then detected and amplified by a 50 GHz bandwidth photodetector. For the measurement of each adjacent pair of signal modes the detuning δ of the optical local oscillator is set to be 7 GHz above the low frequency mode (of the pair). This sets the beat frequency of the local oscillator with the high frequency mode to be ~ 33 GHz. In addition the detector measures the ~ 40 GHz fundamental beat frequency Ω of the signal modes. These last two signals are then mixed with an electronic local oscillator ($f = 30$ GHz) to bring them back into the 10 GHz detection bandwidth of the real-time scope which follows. This mixing is achieved with a single electronic mixer. For higher repetition rate signals multiple electronic mixing stages could be used if necessary. By judicious choice of the detuning of the optical local oscillator, and the frequency of the electronic local oscillator, it is always possible to ensure that these three beat signals all fall within the bandwidth of the realtime scope. This means that the maximum repetition rate of a signal measurable with this system is limited only by the bandwidth of the photodiode and the electronic components preceding the realtime scope, not the bandwidth of the realtime scope itself. The electric field of the signal under test can be written as:

$$E_{sig}(t) = \sum_{m=-N}^N \left(\sqrt{P_m} \exp(jm\Omega t + j\phi_m) \right) \exp(j\omega_s t + j\phi_s(t)) \quad (1)$$

where P_m and ϕ_m are the power and phase of the m^{th} mode, and ω_s and $\phi_s(t)$ represent the optical frequency and phase noise of the carrier. This allows us to write the detected photocurrent after the mixer, when the optical local oscillator is placed between the k^{th} and $k+1$ modes of the optical signal, as:

$$\begin{aligned} S(t) \propto & \sqrt{P_{LO} P_k} \cos(\delta t + \phi_{LO}(t) - \phi_s(t) - \phi_k) \\ & + \sqrt{P_{LO} P_{k+1}} \eta \cos((\Omega - \delta - f)t - \phi_{LO}(t) + \phi_s(t) - \phi_f(t) + \phi_{k+1}) \\ & + A_{fund} \eta \cos((\Omega - f)t - \phi_f(t) + \phi_{fund}) + \text{DC terms} + \text{higher frequency terms.} \end{aligned} \quad (2)$$

where P_{LO} is the power of the optical local oscillator, $\phi_{LO}(t)$ and $\phi_f(t)$ represent the phase noise of the optical local oscillator and the electronic local oscillator respectively, η is the efficiency of the electronic mixer, and A_{fund} and ϕ_{fund} are the amplitude and phase of the fundamental beat signal at Ω . Only the first three terms of Eq. (2) are relevant to the analysis that follows. The acquired digital signal from the real-time scope is processed to recover the 3 electronic beat signals at $\delta = 7$ GHz, $\Omega - \delta - f = 3$ GHz, and $\Omega - f = 10$ GHz. The relative power of the k^{th} signal mode can be determined from the power in the signal at δ . The sensitivity of this power measurement is measured to be $1 \mu\text{W}$ for an optical local oscillator power of 1 mW . The phase difference between the two modes, $\phi_{k+1} - \phi_k$, can be recovered from the phase difference between the signal at $\Omega - f$, and the $\Omega - f$ component of the product of the two beat signals at δ and $\Omega - \delta - f$. As can be seen from Eq. (2) this phase difference is not affected by either phase noise of the signal, or the phase noise of the optical and electronic local oscillators, which all cancel out in the measurement. The optical local oscillator is then stepped across all modes of the signal under test and the measurement repeated at each point. The phase difference between the signal modes can then be integrated to yield a full measurement of the signal's spectral amplitude and phase. From the measurement of the signal's spectral phase it is simple to calculate the signal's group delay via: $GD = -d\phi/d\omega$, and its group delay dispersion via: $GDD = dGD/d\omega$. In Fig. 2 we plot the spectrum of a typical acquisition ($N = 2^{17}$, 40GS/s) when the optical local oscillator is positioned between two 40 GHz signal modes (detuned by + 7 GHz with respect to the low frequency signal mode), and the frequency of the electronic local oscillator in the receiver is set to 30 GHz. The three beat signals at: $\delta = 7$ GHz, $\Omega - \delta - f = 3$ GHz, and $\Omega - f = 10$ GHz are clearly visible. Inset to Fig. (2) is the recovered phase plotted as a function of time. The phase difference used in the reconstruction is the mean of this signal.

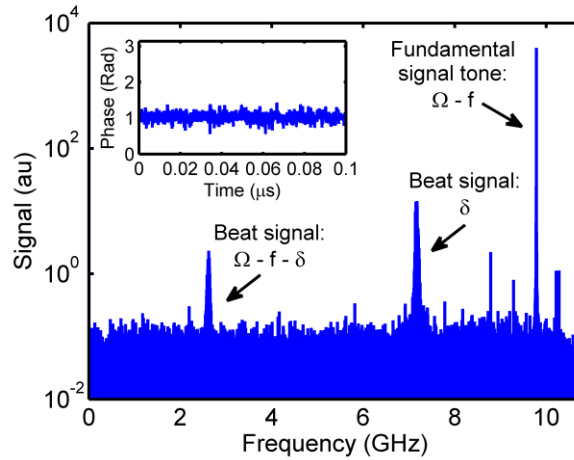


Fig. 2. Spectrum of a typical acquisition of the measurement system with the optical local oscillator positioned between two 40 GHz signal modes. The three required signals at δ , $\Omega - \delta - f$, and $\Omega - f$ are clearly visible. Inset is the recovered phase plotted as a function of time.

3. Experiment

Our first measurement of the spectral amplitude and phase of the free-running QD-MLLD is shown in Fig. 3(a). The DC drive current of the laser diode was 340 mA. The output power of the laser coupled into the fiber is 2 mW. The total length of single mode fiber (SMF-28) in the setup is 9 m. The recovered spectral amplitude and phase of each mode of the spectrum are plotted as circles and diamonds respectively. The laser's spectrum is also measured using a standard grating spectrometer and plotted as a solid line. Good agreement (± 0.5 dB RMS

error) is seen between the power of the spectral modes measured using the stepped-heterodyne technique and the independent measurement made with the grating spectrometer. The spectral phase measurement shows a very strong quadratic dispersion of 2.14 ps^2 across the spectrum. We note that this dispersion does not come from the 9 m of SMF included in the setup which contributes a quadratic dispersion of $\sim -0.17 \text{ ps}^2$, but rather from the laser diode itself. Strong positive quadratic intracavity dispersion has also been observed in lasers of this type in [6]. With the addition of a further length of SMF fiber to the setup it should be possible to compensate this intracavity dispersion. In Fig. 3(b) we plot the stepped-heterodyne measurement of the spectral amplitude and phase of the QD-MLLD at 340mA drive current with an additional 110 m of SMF added to the setup (119 m total). Again, the spectral amplitude and phase of each mode of the spectrum are plotted as circles and diamonds respectively. The solid line shows an independent spectral power measurement made with a grating spectrometer. It can be seen clearly from Fig. 3(b) that the 119 m of SMF has almost completely compensated the strong positive quadratic dispersion of the signal directly exiting the QD-MLLD. The remaining quadratic dispersion is measured to be only -0.03 ps^2 . The residual spectral phase evolution seen in Fig. 3(b) is a result of uncompensated higher order dispersion.

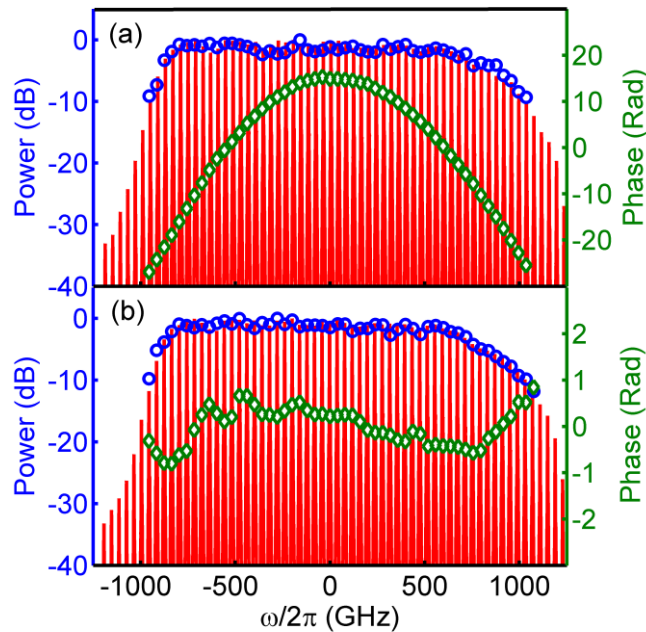


Fig. 3. Measured spectral amplitude and phase of the QD-MLLD at 340 mA drive current. (a) after 9 m of SMF, (b) after 119 m of SMF. The circles and diamonds show the measured spectral amplitude and phase of each laser mode. The solid lines are independent measurements of the laser's spectrum using a grating spectrometer.

From the full measurements of the signal's spectral amplitude and phase shown in Fig. 3 it is simple to reconstruct the signal's temporal amplitude and phase via a Fourier transform. In Figs. 4(a) and 4(b) we plot the temporal amplitude (solid line) and temporal phase (dashed line) reconstructed from the spectral measurements of Figs. 3(a) and 3(b). Figure 4(a) shows the signal after propagation through 9 m of SMF. Due to the strong intracavity dispersion the optical signal is smeared out over the entire 25 ps period with no clear pulse evident. In Fig. 4(b) however the dispersion compensation provided by the 119 m of SMF has transformed the signal into a train of short clean pulses with a FWHM of 490 fs. The small pre-pulses visible in Fig. 4(b) are attributed to incomplete compensation of higher orders of dispersion as shown

in the spectral phase measurement of Fig. 3(b). The time-bandwidth product (TBP) of these pulses is 0.85, compared to a TBP of 0.81 (475 fs pulsewidth) for the same spectrum with a perfectly compensated flat spectral phase.

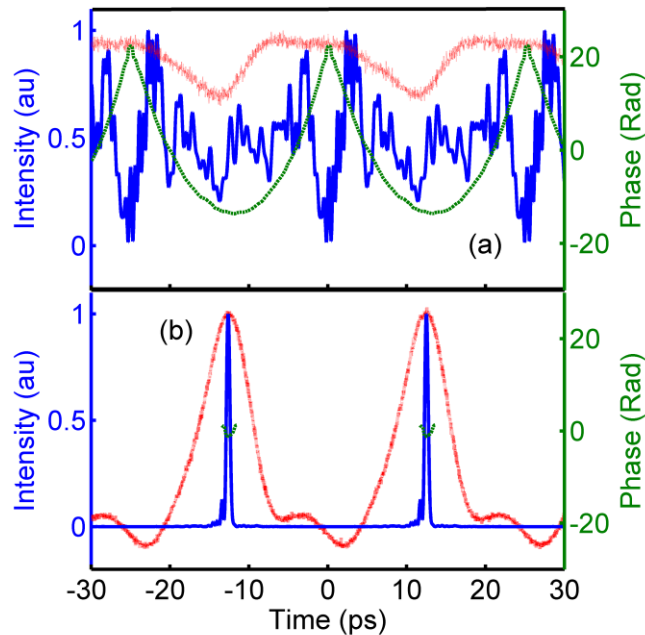


Fig. 4. Temporal amplitude and phase of the QD-MLLD at 340 mA drive current. (a) after 9 m of SMF, (b) after 119 m of SMF. The solid lines and the dashed lines show the temporal amplitude and phase obtained from the spectral amplitude and phase measurements of Fig. 3. The dotted lines show the independent measurement of the intensity profile using a fast photodiode and electronic sampling oscilloscope.

We are unable to measure an autocorrelation trace of the signals shown in Fig. 4. Their broad spectral bandwidth (~ 2 THz) requires the use of a very thin second-harmonic crystal to obtain a phasematching bandwidth that spans the entire signal spectrum. The correspondingly low second-harmonic efficiency of such a crystal, combined with the low average and peak power of the signal under test (~ 2 mW and 100 mW respectively for the pulse shown in Fig. 4(b)) prevent us from measuring an autocorrelation trace of these signals. Instead we measure the temporal intensity profiles of the laser diode's output using a 65 GHz electronic sampling scope and a photodiode with a 7 ps rise time. These measurements are plotted as dotted lines in both Figs. 4 (a) and (b). Although limited by the temporal response of the photodiode these traces clearly confirm the absence of any optical pulse after 9 m of fiber, and the presence of a pulse after 119 m. As an additional check on the reliability of these measurements we can compare the temporal intensity trace measured after 119 m of SMF, with the temporal intensity trace of the signal measured after 9 m of SMF with the dispersion of the additional 110 m of SMF applied numerically. The level of agreement between these two independent measurements gives a quantitative indication of the technique's accuracy. The magnitude of the numerical dispersion compensation applied is set by the difference between the quadratic dispersions measured after 9 and 119 m of SMF. From Figs. 3(a) and 3(b) this difference is measured to be: $-0.03 \text{ ps}^2 - 2.14 \text{ ps}^2 = -2.17 \text{ ps}^2$. The optical fiber also possesses a third-order dispersion component of $\sim 0.15 \text{ ps}^3/\text{km}$, which we also include in our numerical dispersion compensation, however we find its effect on the temporal pulse shape is almost negligible. In Fig. 5(a) we plot the temporal intensity trace calculated from the spectral amplitude and phase measurement made after 119 m of SMF, in Fig. 5(b) we plot the temporal intensity trace calculated from the spectral amplitude and phase measurement made after 9 m of SMF with

the dispersion of the additional 110 m of SMF applied numerically. The agreement between these two independent measurements is very good with both showing clean pulses of ~ 500 fs FWHM (490 fs for Fig. 5(a), and 530 fs for Fig. 5(b)). As well as the temporal comparison of the two pulses shown in Fig. 5 we can compare the spectral phase of these two signals which allows us to estimate the experimental error for our spectral phase measurement. From the difference between the spectral phases of the two traces shown in Fig. 5 we calculate an RMS spectral phase error for the measurement of 0.2 radians.

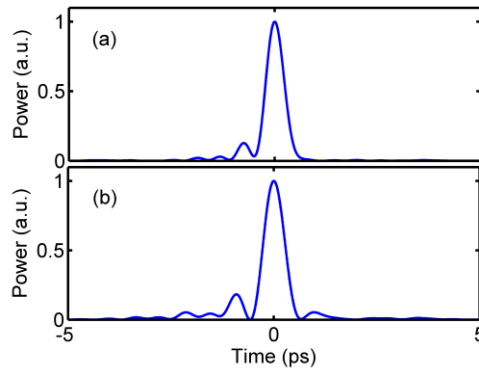


Fig. 5. (a) Temporal intensity trace of the pulse measured after 119 m of SMF (Fig. 4(b)). (b) Temporal intensity trace of the pulse measured after 9 m of SMF (Fig. 4(a)) with the dispersion of the additional 110 m of SMF applied numerically.

To demonstrate the utility of the stepped-heterodyne measurement in characterizing the optical properties of the QD-MLLD output we next measure the intracavity dispersion of the laser as a function of drive current. In Fig. 6(a) we plot the spectral amplitude and phase of the output of the laser, measured after 9 m of SMF, at drive currents of 140, 240 and 340 mA. These measurements show that reducing the drive current of the laser actually increases the quadratic dispersion of the signal. Quantitatively we measure 2.58, 2.26 and 2.14 ps² of quadratic dispersion at drive currents of 140, 240 and 340 mA respectively. A consequence of this change in signal dispersion with drive current is that the 119 m SMF fiber length used to compensate the laser's intracavity dispersion at 340 mA will not correctly compensate the output pulse at other currents. We demonstrate this in Fig. 6(b) where we plot the temporal intensity profile of the pulse, calculated from a spectral measurement, after propagation through 119 m of SMF at drive currents of 140, 240 and 340 mA. The output pulses at 140 and 240 mA can be clearly seen to have broken up due to imperfect dispersion compensation. We calculate the correct fiber lengths required to fully compensate the output of the laser at these currents to be 143 and 126 m respectively.

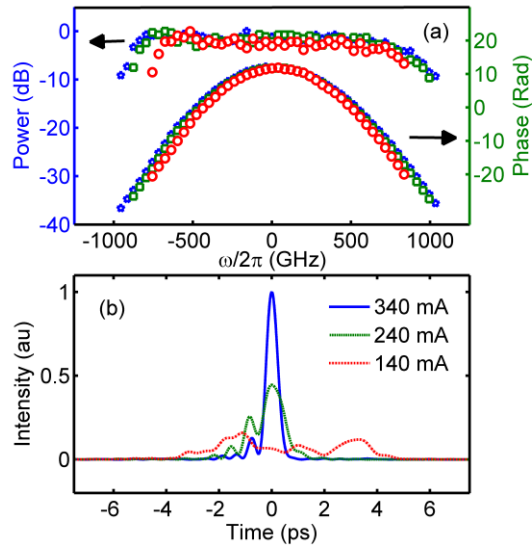


Fig. 6. (a) Measured spectral amplitude and phase of the QD-MLLD after 9 m of SMF at 340 mA (stars), 240 mA (squares) and 140 mA (circles). (b) Measured temporal intensity profile of QD-MLLD pulse after 119 m of SMF at 340 mA (solid line), 240 mA (dotted line) and 140 mA (dashed line).

4. Conclusion

In conclusion we have demonstrated a linear self-referenced measurement of the spectral amplitude and phase of a QD-MLLD. In contrast to the previously demonstrated FROG characterization of this device this method allows the undistorted measurement of the spectral and temporal amplitude and phase characteristics of the laser both before and after dispersion compensation is applied. The technique is capable of measuring repetition rates up to 100 GHz and does not require any synchronized electronic clock to operate. With correct dispersion compensation we observe 500 fs pulses at a repetition rate of 39.8 GHz from a free-running QD-MLLD. We have also used the measurement to characterize the intracavity dispersion of the laser as a function of injection current.

Acknowledgments

This work was supported by the High Education Authority via the INSPIRE program and by Science Foundation Ireland through the Principle Investigator program.